Asymmetry dependence of neutron correlations in Ar isotopes

Jenny Lee(李曉菁)[1], M.B. Tsang(曾敏兒)[1], D. Bazin[1], D. Coupland[1], V. Henzl[1], D. Henzlova[1], M. Kilburn[1], W.G. Lynch(連致標)[1], A. Rogers[1], A. Sanetullaev[1], A. Signoracci[1], Z.Y. Sun(孙志宇)[1,2] , M. Youngs[1], K.Y. Chae[3], R.J. Charity[4], H.K. Cheung (張凱傑)[5], M. Famiano[6], S. Hudan[7], P. O'Malley[8], W.A. Peters[8], K. Schmitt[3], D. Shapira[9], L.G. Sobotka[4]

[1]*NSCL & Department of Physics and Astronomy, Michigan State University, East Lansing, MI 48864, USA*
[2]*Institute of Modern Physics, CAS, Lanzhou 730000, People's Republic of China*
[3]*Department of Physics and Astronomy, University of Tennessee, Knoxville, Tennessee 37996, USA*
[4]*Department of Chemistry, Washington University, St. Louis, MO 63130, USA*
[5]*Physics Department, Chinese University of Hong Kong, Shatin, Hong Kong, China*
[6]*Department of Physics, Western Michigan University, Kalamazoo, MI 49008, USA*
[7]*Department of Chemistry, Indiana University, Bloomington, IN 47405, USA*
[8]*Department of Physics and Astronomy, Rutgers University, Piscataway, New Jersey 08854-8019, USA*
[9]*Oak Ridge National Laboratory, Oak Ridge, TN 37831, USA*

Abstract

Both nucleon transfer and knockout reactions are expected to be reliable probes of spectroscopic factors, hence reflect the effects of nuclear asymmetry. To explore the dependence of neutron correlations on nuclear asymmetry, spectroscopic factors have been measured for proton rich ^{34}Ar and neutron rich ^{46}Ar using the (p,d) neutron transfer reaction. The experimental results show no extra reduction of the ground state neutron spectroscopic factor of the proton rich nucleus ^{34}Ar compared to that of ^{46}Ar. The results suggest that neutron correlations, which generally reduce such spectroscopic factors, do not depend strongly on the asymmetry of the nucleus in this isotopic region. The present results are consistent with results from systematic studies of transfer reactions and from global analyses of $^{40\text{-}49}$Ca scattering data via the dispersive optical-model, but inconsistent with the systematic trends of knockout reaction measurements.

As Fermi liquids, the interactions and the correlations between the nucleon constituents in a nucleus have a profound effect on nuclear properties [1,2]. Short-range correlations between nucleons mitigate their strong short-range repulsion and reduce their bulk compressibility, key to stability of neutron stars against collapse into black holes [3]. Long-range pairing correlations between valence nucleons in a nucleus couple pairs of valence neutrons or protons to spin zero and are analogous to superconductivity and superfluidity in macroscopic systems [4,5]. Long range correlations also result in collective modes that, along with pairing correlations, strongly influence the spectrum of excitations near the Fermi surface and the heat capacity, consequences well known in nuclei and other Fermi liquids such as liquid ^{3}He [1,2].

Both long and short range correlations spread the contributions from single-particle orbits over a large range in excitation energy [6]. This can be probed by measuring spectroscopic factors, which describe the contributions of specific single-particle orbits to specific states. Measurements of proton spectroscopic factors near closed shell nuclei using (e,e'p) reactions indicate that correlations typically reduce valence orbital occupancies by about 30-40% [7]. Some of the correlations arising from the long-range components of the interaction, which induces couplings to the low-lying collective excitation and giant resonances, can be described within current shell models [6,8]. The nature of such long-range correlations may vary strongly from nucleus to nucleus. Properties of the remaining long-range correlations as well as correlations due to the higher momentum short-range and tensor parts are under active investigations [6,7,9].

Measurement of single-nucleon removal mechanisms, such as single-nucleon transfer or knockout, provide constraints on spectroscopic factors (SF's) calculated from the overlap between many-body wave functions of the initial and final states [10]. Together with the studies in stable nuclei, measurements with rare isotope beams allow one to determine how SF's depend on the asymmetry of the system for nuclei ranging from stability to the drip lines. Large reductions (up to 75%) in the measured SF values relative to shell model predictions have been observed in one-nucleon knockout reactions for strongly bound valence neutrons (in proton-rich nuclei) and strongly bound valence protons (in neutron-

rich nuclei) [11]. Such large reductions in spectroscopic factors suggest qualitatively new phenomena may play a role in the two component (neutron and proton) Fermi liquids. Even though the strength of these reductions for strongly bound minority constituents in nuclear systems is not theoretically anticipated, some studies do predict smaller effects [6,7,9,12,13]. Dispersive Optical Model (DOM) results which include the effects of long-range correlations, predict changes in the proton SF magnitudes from ^{40}Ca to ^{49}Ca of about10%, for example [13]. These latter changes reflect the couplings of the specific single-particle orbits to low lying collective excitations and may differ in other regions of the nuclear mass and charge.

In this paper, we investigate these effects using an alternative spectroscopic probe: (p,d) single-nucleon transfer reactions. Recently, a consistent and systematic understanding of SF's from single neutron transfer was conducted for (p,d) and (d,p) reactions by comparing cross-section data to calculations [14] based on the Johnson-Soper Adiabatic Distorted Wave Approximation (ADWA) [15] and nucleon global elastic scattering optical potentials [16,17]. Utilizing the Chapel-Hill (CH89) nucleon-nucleus global optical potential [18] and a neutron potential with fixed radius and diffuseness parameters, r_0=1.25 and a_0=0.65 fm, agreement to within 20% between measured neutron SF's and those calculated via Large Basis-Shell Model's (LB-SM) for ground states with $3 \leq Z \leq 28$ [19, 20] is observed. For most excited states of stable nuclei with $3 \leq Z \leq 24$, the agreement is slightly worse, to within 30%. If the JLM global optical model [21] with the conventional scale factors for the computed real and imaginary part of $\lambda_V = 1.0$ and $\lambda_W = 0.8$ [22] is used with its geometry and that for the transferred-neutron bound state constrained by Hartee-Fock calculations[23], we observe an overall reduction ~30% in the measured ground state spectroscopic factors compared to LB-SM predictions [24]. The reduction factor *Rs* ≡ (experimental SF)/(theoretical SF) in the latter approach is similar to that observed for proton SFs obtained in (e,e'p) measurements [25].

Regardless of the choice of optical model potential or the geometry of the mean field potential for the transferred neutron, these systematic analyses of neutron transfer reactions displayed no strong dependence of the reduction factor *Rs* on the asymmetry of

the target or the difference between valence neutron and proton separation energies [19,20,24]. This suggests a relatively weak asymmetry dependence of the neutron correlations over the range of asymmetry that stable beam experiments have explored. However, the available data includes very few extremely neutron-rich or neutron-deficient nuclei. In addition, systematic uncertainties inherent in comparing SF's from different experiments published over a period of more than 40 years reduce the sensitivity of such studies to the smaller effects expected for stable nuclei.

To explore more extreme asymmetries, we measured neutron transfer reactions using proton rich ^{34}Ar and neutron rich ^{46}Ar beams in inverse kinematics and extracted the experimental ground-state neutron SF's for ^{34}Ar and ^{46}Ar. SF's from knockout reactions on these nuclei have been published and a significant reduction of the neutron SF for ^{34}Ar has been reported. [11]. The difference between the neutron and proton separation energy (ΔS), which characterizes the relative shift of neutron and proton Fermi energies in these nuclei, is 12.41 MeV and -10.03 MeV for ^{34}Ar and ^{46}Ar respectively. In previous studies of transfer reactions, there were no nuclei with $|\Delta S| >> 7$ MeV [19, 24].

In the present experiment, p(^{34}Ar,d) ^{33}Ar and p(^{46}Ar,d) ^{45}Ar transfer reactions were measured using radioactive secondary beams of ^{34}Ar and ^{46}Ar beams at 33 MeV/nucleon at the National Superconducting Cyclotron Laboratory at Michigan State University [26]. The ^{34}Ar and ^{46}Ar beams were produced by fragmenting 150 MeV/nucleon ^{36}Ar and 140 MeV/nucleon ^{48}Ca primary beams, respectively and identified unambiguously by the time of flight between the K1200 cyclotron (using the radio-frequency) and a plastic scintillator placed at the focal plane of the A1900 fragment separator [27]. The p(^{36}Ar,d) ^{35}Ar reaction was also measured using a degraded ^{36}Ar primary beam at 33MeV/nucleon for comparison with data previously measured in normal kinematics [28].

These beams were transported to the S800 target where they were focused on CH_2 targets, with areal densities of 7.10 mg/cm^2 for ^{34,36}Ar and 2.29 mg/cm^2 for ^{46}Ar reactions. The averaged beam intensities on target were monitored by a Micro-Channel Plates (MCP) tracking detector [29,30] that was placed ~10 cm upstream of the target. Both the

deuteron and the ^{33}Ar, ^{35}Ar or ^{45}Ar residues were detected in a kinematically complete measurement; the deuterons were detected in the High-Resolution Array (HiRA) [31] and the recoil residues were detected in the S800 focal plane [32,33]. An array of 16 HiRA telescopes [31] were placed 35 cm from the target where they subtended polar angles of $4° \leq \theta_{lab} \leq 45°$. Each telescope contained 65μm thick ΔE and 1500 μm thick E silicon strip detectors, backed by 3.9 cm thick CsI(Tl) crystals. The strips in these telescopes effectively subdivided each telescope into 1024 2mmx2mm pixels, each with an angular resolution of about ±0.16°. Detailed descriptions of experimental setup can be found in Ref. [26].

Deuterons were identified in HiRA with standard energy loss techniques using the energy deposited in the ΔE and E Silicon strip detectors and CsI detectors. Reaction residues were identified in the S800 using the energy loss in the ionization chamber and the time-of-flight. For the coincidence events, the reaction Q value was determined from the energy and angle of the detected deuteron on an event-by-event basis. The Q value spectra which exclude events of deuterons punching though the thick Si detector for p(^{34,36,46}Ar,d)^{33,35,45}Ar are shown in Figs. 1(a-c). The resolutions coming from the finite beam spot size and the energy resolution of the Si detectors, energy loss in the target and angular straggling in the target, are obtained using GEANT4 [34] simulations. The results agree with the observed resolutions of 500, 470 and 410 keV FWHM for the transitions to the ground-states of ^{33,35,45}Ar respectively. Measurements performed using a 1.7 mg/cm^2 carbon target reveal that by detecting both deuteron and heavy recoil, the background is reduced to a negligible level. The absolute normalization of the cross section was achieved to within 10% by directly counting the beam particles with the MCP in front of the reaction target.

Figs. 1(d), 1(e) and 1(f) show the differential cross sections for the ground-state transition of p(^{34}Ar,d)^{33}Ar, p(^{36}Ar,d)^{35}Ar, and p(^{46}Ar,d)^{45}Ar, respectively. The solid circles denote the data from present measurement in inverse kinematics and the open squares in Fig. 1(e) denote the previous ^{36}Ar (p,d)^{35}Ar data in normal kinematics at 33.6MeV/nucleon [28]. The agreement between the measured cross-sections from the

present work and Ref. [28] for the first excited-state is also very good [26]. For p(^{46}Ar,d)^{45}Ar reaction, the ground state and the first excited state (542 keV) cannot be resolved for center-of-mass angles larger than 8°. Fortunately, the *l* values for the ground state (*l*=3) and first excited state (*l*=1) are different, resulting in very different angular distributions. Specifically, the angular distribution for the excited state exhibits a deep minimum near θ_{CM} =20-27 °, close to a factor of 100 smaller than that of ground state; there, the cross-sections for the ground state were also unambiguously extracted[26].

The dot-dash lines in Figs. 1(d-f) show the ADWA calculations using the CH89 potential with the conventional neutron bound-state Woods-Saxon potential parameters, r_0=1.25 and a_0=0.65fm. The solid lines in Figs. 1(d-f) show the ADWA calculations using the JLM microscopic potential [21] and the bound-state neutron potential, which have been constrained by Hartree-Fock calculations [23]. Both CH89 and JLM calculations reproduce the shape of experimental angular distributions. Normalizing the ADWA model calculations to the data results in the SF values listed in Table 1. Similar to previous analysis, SF(JLM+HF) values are smaller than the SF(CH89) values. The ground-state neutron SF's for ^{34}Ar and ^{36}Ar were calculated in the sd-shell model space with the Oxbash code [35] using USDB effective interaction [36]. The ground-state neutron SF for ^{46}Ar was calculated in the sd-pf model space using the interaction of Nummela et al [37]. The calculated SF values are presented in Table 1.

The ground-state reduction factors *Rs,* defined as the ratio of the experimental SF value divided by the LB-SM prediction are listed in Table 1. In Figure 2, *Rs* are plotted as a function of the difference in the neutron and proton separation energies, ΔS, as open circles (*Rs*(CH89) = SF(CH89)/SM(LB-SM)) and closed circles (*Rs*(JLM+HF) = SF(JLM+HF)/SM(LB-SM)). The error bars listed in Table 1 and associated with the open circles in Fig 2 reflect the uncertainties in the absolute cross-section determination [26]. (For clarity of presentation, the error bars for the closed circles are not plotted.) In both cases, the value of *Rs* for proton-rich ^{34}Ar is consistent with the values of *Rs* for symmetric ^{36}Ar, for neutron-rich ^{46}Ar and the values for stable nuclei included in the previous analysis [19,20,24]. The dot-dash and solid lines represent their average value.

The weak dependence,(<12%), of reduction factors on the asymmetry of the three Ar isotopes is similar to the trends obtained from the recent DOM analysis of elastic-scattering and bound-level data for $^{40-49}$Ca isotopes [13]. In contrast, a much larger systematic suppression in SFs has been reported for the knockout reactions [11], when the removed nucleon has a large separation energy. As shown by the open triangles in Fig. 2, the neutron *Rs* extracted from knockout reactions for ^{34}Ar is approximately a factor of two smaller than that for ^{46}Ar. Even larger reductions have been observed for neutron knockout from ^{32}Ar, a nucleus for which transfer data is not available. This suggests that there is a systematic difference between the conclusions drawn from these two probes for the spectroscopic factors of strongly bound particles. Thus a reexamination of the reaction theory description of transfer reactions or knockout reactions including the input parameters used in these analyses may be needed.

In summary, we have extracted the neutron ground-state spectroscopic factors of proton-rich ^{34}Ar and neutron rich ^{46}Ar using (p,d) transfer reactions with radioactive beams in inverse kinematics. The experimental results, analyzed with two different approaches using different optical model potentials and different neutron bound-state geometries, are consistent with extensive systematics of spectroscopic factors obtained from transfer reactions on stable nuclei. We do not observe a significant difference in the reduction factors for the spectroscopic factors for ^{34}Ar and ^{46}Ar suggesting a weak dependence of neutron correlations on asymmetry in this nuclear region. Such observation agrees with that obtained from dispersive-optical model analyses of elastic scattering and bound state data for Ca isotopes. Unlike the trends observed for knockout reactions, we do not observe a strong dependence of these reduction factors on the difference between neutron and proton separation energies. These new results examine the nature of neutron correlations in nuclei with unusual isospin asymmetries while posing questions about the reaction mechanisms of transfer and knockout reactions used to probe them.

Acknowledgement

The authors would like to thank Professors B.A. Brown and J. Tostevin for the use of the programs Oxbash and TWOFNR. This work is supported by the National Science Foundation under grants PHY-0606007. Cheung acknowledges the support of the Summer Undergraduate Research Experience (SURE) program sponsored by the Chinese University of Hong Kong. Sun acknowledges support from MSU during his stay at NSCL in 2008.

Reference

[1] D. Pines and P. Nozières, *The Theory of Quantum Liquids*, Benjamin, New York (1966).

[2] G. Baym and C. Pethick, *Landau Fermi-liquid Theory*, Wiley-VCH Verlag GmbH & Co. KGaA, Weinheim (2004).

[3] H. Heiselberg and M. Hjorth-Jensen, Phys. Rep. 328, 237 (2000).

[4] M. A. Preston and R. K. Bhaduri, *Structure of the Nucleus*, Addison-Wesley Pub. Co. Boston (1974).

[5] W. H. Dickhoff and D. V. Neck, *Many-body theory exposed*, World Scientific, Singapore (2008)

[6] W. H. Dickhoff and C. Barbieri, Prog. Part. Nucl. Phys. 52, 377 (2004).

[7] V. R. Pandharipande et al., Rev. Mod. Phys. 69, 981 (1997).

[8] B. A. Brown, Prog. Part. Nucl. Phys. 47, 517 (2001).

[9] C. Barbieri, arXiv:0909.3040v1 [nucl-th] (2009).

[10] N. Austern, *Direct Nuclear Reaction Theories*, John Wiley & Sons, New York (1970).

[11] A. Gade et al., Phys. Rev. C77, 044306 (2008) and reference therein.

[12] T. Frick et al., Phys. Rev. C71, 014313 (2005).

[13] R. J. Charity et al., Phys. Rev. C76, 044314 (2007).

[14] M. Igarashi, et al., M. Toyoma and N. Kishida, Computer Program TWOFNR (Surrey University version).

[15] R. C. Johnson and P. J. R. Soper, Phys. Rev. C 1, 976 (1970).

[16] X. D. Liu et al., Phys. Rev. C **69**, 064313 (2004).

[17] J. Lee et al., Phys. Rev. C **75**, 064320 (2007).

[18] R. L. Varner et al., Phys. Rep. **201**, 57 (1991).

[19] M. B. Tsang et al, Phys. Rev. Lett. 95, 222501 (2005).

[20] M. B. Tsang et al., Phys. Rev. Lett. 102, 062501 (2009).

[21] J.-P. Jeukenne et al., Phys. Rev. C1, 976 (1970).

[22] J. S. Petler et al., Phys. Rev. C32, 673 (1985).

[23] B. A. Brown, Phys. Rev. C58,220 (1998).

[24] J. Lee et al, Phys. Rev. C73, 044608 (2006).

[25] G.J. Kramer et. al., Nucl. Phys. A. 679, 267 (2001) and references therein.

[26] J. Lee, PhD thesis, Michigan State University (2009).

[27] D. J. Morrissey et al., Nucl. Instrum. Methods B 204, 90 (2003).

[28] R. L. Kozub, Phys. Rev. 172, 1078 (1968).

[29] D. Shapira et al., Nucl. Inst. and Meth. A. 449, 396 (2000).

[30] D. Shapira et al., Nucl. Inst. and Meth. A. 454, 409 (2000).

[31] M. S. Wallace et al., Nucl. Instrum. Methods Phys. Res. A583, 302 (2007)

[32] J. Yurkon et al., Nucl. Instrum. Methods Phys. Res., Sect. A 422, 291 (1999).

[33] D. Bazin et al., Nucl. Instrum. Methods Phys. Res. B 204, 629 (2003).

[34] S. Agostinelli et al., Nucl. Instrum. Meth. A, 506, 250 (2003).

[35] B. A. Brown et al., Computer program,

http://www.nscl.msu.edu/~brown/resources/resources.html.

[36] B. A. Brown et al, Phys. Rev. C74, 034315 (2006).

[37] A. Signoracci and B. Alex Brown, Phys. Rev. Lett. 99, 099201 (2007).

[38] R. J. Charity and L.G. Sobotka (private communication).

[39] In this work, the ground state to ground state transition cross sections are determined but in Ref. [11], inclusive cross sections with contributions from the excited states to the ground states were measured. Thus the ^{34}Ar ΔS value in Ref. [11] is weighted by the nucleon separation energy of the excited states. In principle, the knockout value should give the upper limit of the ^{34}Ar ground-state *Rs* value as contributions from excited states would increase the reduction factor.

Fig. 1. (Color online) Q-value spectrum (a-c, top panels) and deuteron angular distributions (d-f, bottom panels) to ground state of p(^{34,36,46}Ar,d)$^{33,\ 35,\ 46}$Ar. In (e, bottom middle panel) the open squares are the data from previous normal kinematics experiments [28]. The solid and dot-dash lines represent the calculations using JLM+HF and CH89 approach respectively.

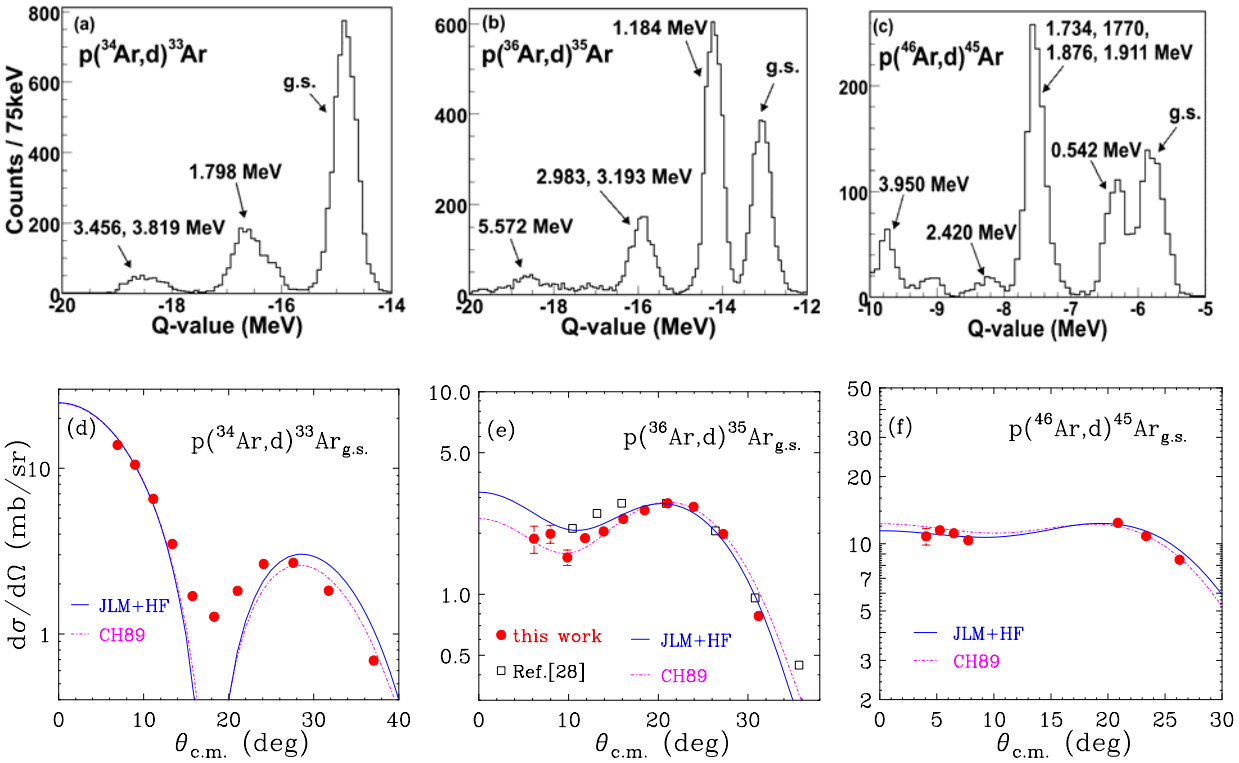

Fig. 2. (Color Online): Reduction factors *Rs*=SF(expt)/SF(LB-SM) as a function of the difference between neutron and proton separation energies, ΔS. The solid and open circles represent the *Rs* deduced in JLM+HF and CH89 approach using the present transfer reaction data respectively. The open triangles denote the *Rs* from knockout reactions [11]. The solid and dot-dash lines are the averaged *Rs* values from the present work, while the dashed line is the best fit of *Rs* of ^{32,34,46}Ar from knockout reactions. The use of different ΔS values from the present work and Ref. [11] is explained in Ref. [39].

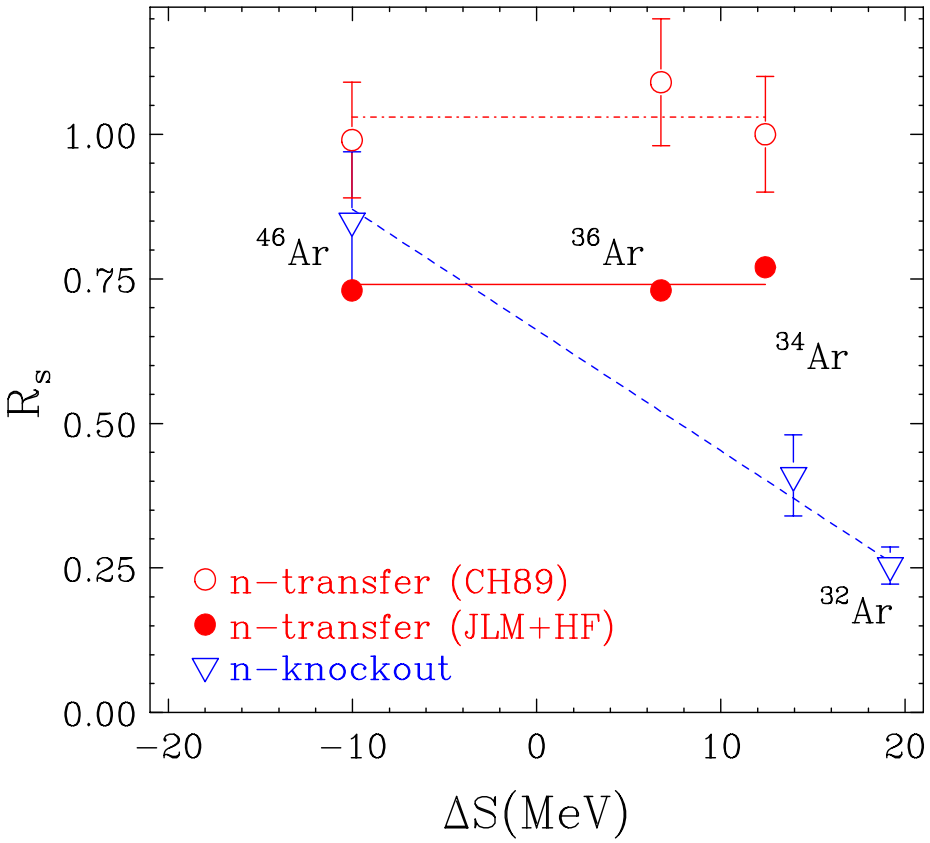

Table 1. Experimental and theoretical neutron spectroscopic factors (SF) and reduction factors (*Rs*) for ground state ^{34}Ar, ^{36}Ar and ^{46}Ar.

Isotopes	lj^{π}	Sn(MeV)	ΔS (MeV)	(theo.)	(expt.)		(expt.)	
				SF(LB-SM)	SF(JLM+HF)	Rs(JLM+HF)	SF(CH89)	Rs(CH89)
^{34}Ar	s1/2^{+}	17.07	12.41	1.31	1.01±0.10	0.77±0.08	1.31±0.13	1.00±0.10
^{36}Ar	d3/2^{+}	15.25	6.75	2.10	1.53±0.15	0.73±0.07	2.29±0.23	1.09±0.11
^{46}Ar	f7/2^{-}	8.07	-10.03	5.16	3.77±0.38	0.73±0.07	5.13±0.51	0.99±0.10